Journal of New Materials for Electrochemical Systems 8, 317-325 (2005)

Phase Transitions of the WO_3 Layer in Photoelectrochromic Devices

Anneke Georg[1*], Andreas Georg[2], Urša Opara Krašovec[3], Volker Wittwer[2]

[1]*Freiburg Materials Research Centre, Stefan Meier Str. 21, 79104 Freiburg, Germany*
[2]*Fraunhofer Institute for Solar Energy Systems, Heidenhofstr. 2, 79100 Freiburg, Germany*
[3] *Faculty of Electrical Engineering, University of Ljubljana, Tržaška 25, SI-1000 Ljubljana, Slovenia*

(Received May 30, 2005 ; received in revised form March 9, 2006)

Abstract: *Photoelectrochromic systems are a combination of a dye solar cell and an electrochromic material, usually WO_3. They change their transmittance on illumination. We prepared a particularly advantageous configuration, which can be coloured and bleached under illumination, and bleached in the dark. During colouring, electrons and Li^+ cations are intercalated into the electrochromic WO_3 layer. Due to this intercalation, the WO_3 crystals change their structure from monoclinic through tetragonal to cubic. The intercalation and the phase transition are completely reversible. We investigated these phase transitions with the help of electrochemical potential measurement, IR spectroscopy and X-ray diffractometry, applied to the separate layers. We discuss the effect of the phase transition on the colouring and bleaching characteristics of the photoelectrochromic device, i.e. the time dependence of the voltage and the optical density.*

Key words : photoelectrochromic, electrochromic, window, WO_3, phase transition

1. INTRODUCTION

1.1 Related Work of Other Authors About Phase Transitions in WO_3

Zhong et. al reported [11] the phase transition of monoclinic polycrystalline evaporated WO_3 layers occurring during electrochemical intercalation of Li^+. They used sealed cells with Li foil as the anode and WO_3 evaporated onto Be foil as the cathode, and an electrolyte of 1 M $LiClO_4$ dissolved in a mixture of propylene carbonate and ethylene carbonate. The voltage (V) of the cell corresponds to the electrochemical potential of WO_3 versus Li. The voltage (V) was measured as a function of the degree of intercalation x (x = number of intercalated Li^+ cations per W atom) during galvanostatic charging and discharging under equilibrium conditions. In-situ X-ray diffraction (XRD) measurements were taken during charging and discharging. The analysis of V(x) and XRD measurements gave a phase diagram of Li intercalation/extraction in WO_3: With increasing x, the initially monoclinic WO_3 changes to crystal structures of higher symmetry: first it transforms to tetragonal Li_xWO_3, then to the cubic Li_xWO_3phase. The phase transitions are completely reversible. The V(x) curve has a step corresponding to each phase transition. During the coexistence of two phases, V(x) shows a plateau. In a pure phase, V decreases with increasing x. The phase transition starts with a critical value of x, which is not the same for charging and discharging. The V(x) versus Li is always lower during charging than during discharging.

1.2 Working Principle of Photoelectrochromic Devices

Photoelectrochromic systems combine electrochromic layers [1, 2] and dye solar cells [3, 4]. Electrochromic layers change their transmittance reversibly when electrons and cations are injected. In photoelectrochromic systems, the dye solar cell provides the energy for the coloration of the electrochromic layer. Thus the transmittance of the photoelectrochromic device

*To whom correspondence should be addressed: Anneke Georg, Freiburg Materials Research Centre, Stefan-Meier-Str. 21, 79104 Freiburg, Germany, phone: ++49 (0) 761 203 4799, fax: ++49 (0)761 2034801, email: anneke.georg@fmf.uni-freiburg.de

can be decreased under illumination and can be increased again when in the dark. An external voltage supply is not required. Applications of these devices include, for example, switchable sunroofs in cars or smart windows in buildings.

We developed the photoelectrochromic configuration illustrated in fig.1, which is a particularly advantageous device. It consists of several components (fig.1): a dye-covered nanoporous TiO_2 layer, a porous electrochromic layer, such as WO_3, two glass substrates coated with a transparent conductive oxide (TCO), of which one is coated with Pt, an iodide/triiodide redox couple and Li^+ ions in an organic solvent. Both the TiO_2 and the Pt layers can be kept thin, so that the electrodes remain transparent. The pores of the TiO_2 and WO_3 layers are filled with the electrolyte.

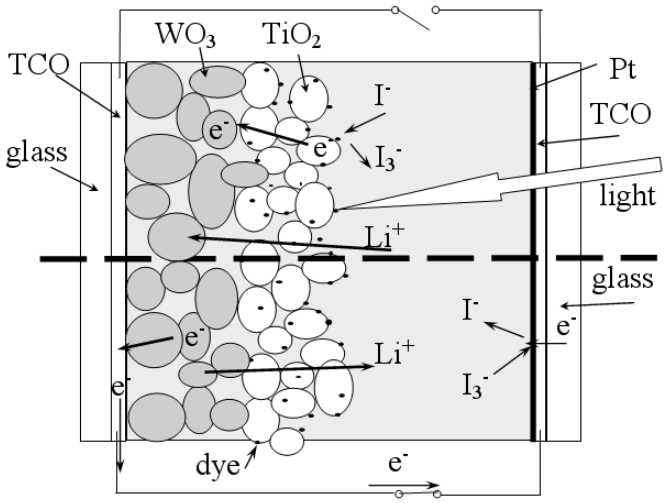

Figure 1: Construction and operating principle of the photoelectrochromic device. The upper part shows the coloration in open circuit (switch open) and the lower part the bleaching in short circuit (switch closed).

During illumination (upper part of fig.1), a dye molecule absorbs a photon of the incident light. Then an electron is rapidly injected from the excited state of the dye into the conduction band of the TiO_2 and diffuses to the WO_3. Ionised dye molecules are reduced by receiving electrons from I^- present in the electrolyte according to the reaction: $2dye^+ + 3I^- \rightarrow I_3^- + 2dye$. Lithium cations intercalate into the WO_3 and keep the charges balanced. Because of the injection of electrons, the WO_3 is reduced and changes its colour from colourless to blue.

If electrons are allowed to flow via an external circuit from the WO_3 via a TCO layer to the Pt electrode (lower part of fig.1, external switch closed), then the Pt catalyses the reverse reaction, i.e. the reduction of I_3^- to I^-. Lithium cations leave the WO_3, and the WO_3 bleaches fast. This process occurs also during illumination. If the external switch is open, electrons can leave the WO_3 only by loss reactions. This process is very slow.

1.3 Properties of the Photoelectrchromic Device

If the electrolyte is liquid, the photoelectrochromic device's visible (solar) transmittance changes under 1000 W/m^2 of illumination (1 sun) from 51% to 5% (35% to 1.5%) with switching times of about 3 minutes (fig. 2). With a solid electrolyte, a visible transmittance change from 62% to 1.6% and a solar transmittance change from 41% to 0.8% are achieved with switching times of 10 min. The colouring time is independent of the area.

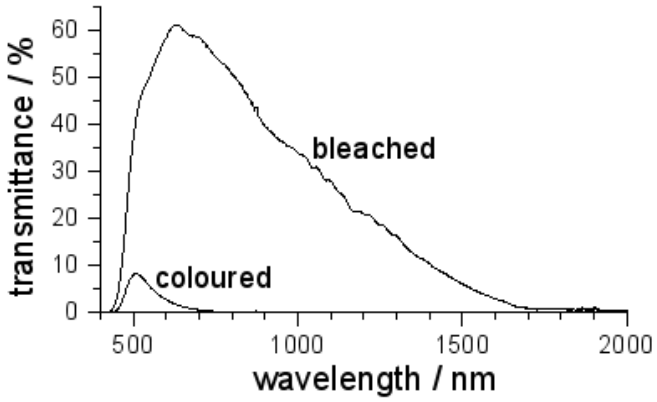

Figure 2: Transmittance spectra of the photoelectrochromic device in the coloured and bleached states. For a cell with liquid electrolyte the visible (solar) transmittances changes from 51% (35%) to 4.8% (1.5%) in 3 min.

In contrast to an alternative photoelectrochromic configuration [5, 6, 7], this device allows simultaneously fast colouring and bleaching and a high contrast [8], and the transmittance can be varied also in the illuminated state. Furthermore, in contrast to photochromic devices, the system is externally switchable.

This new device was introduced in our previous paper [8]. The paper discussed the differences to the alternative photoelectrochromic system and the advantages of our new system. Experiments with different layer configurations of photoelectrochromic devices are investigated in Ref. [9].

1.4 Previous Work on our WO_3 - and TiO_2- Layers, Comparison with and Introduction to the Present Work

We developed special nanoporous WO_3 and TiO_2 layers for the photoelectrochromic system. The structure and morphology of our WO_3-TiO_2 layers was assessed with high-resolution transmittance electron spectroscopy (HRTEM), IR spectroscopy, Auger electron spectroscopy and energy-dispersive X-ray spectroscopy (EDXS) [10]. The result was that the particles in the WO_3 layer are about 20 – 30 nm in diameter and consist of

a crystalline monoclinic WO_3core, which is surrounded by an amorphous phase (fig. 3). The amorphous phase consists of WO_3, TiO_2 (20% of metal atoms in WO_3 layer are Ti) and some SiO_2 (2% mol. relative to W) which has remained from the preparation process.

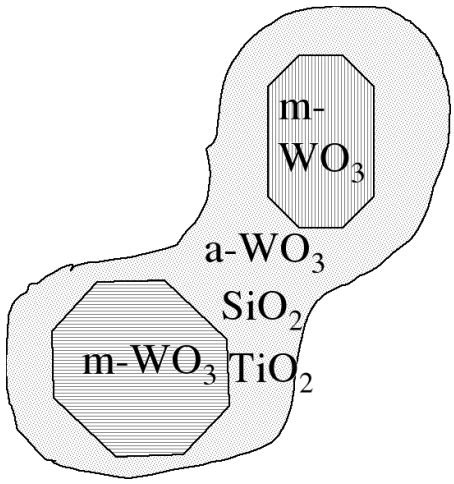

Figure 3: Result of the structural investigation of the WO_3 layer (REM, Auger, HRTEM, EDXS).

The phase transitions of crystalline sol-gel WO_3 layers during charge intercalation have been studied also by using ex-situ IR spectroelectrochemical measurements [12]. Additionally, ex-situ XRD spectra were taken before and after coloration of the layers. These XRD spectra identified monoclinic crystal structure of the WO_3 layers before and cubic structure after coloration (x$\approx$ 0.3) [12].

The sol-gel process for the preparation of the WO_3 layers [12] was the same as for the WO_3 in the photoelectrochromic device, except for the addition of the binder: In Ref. [12] no binder was added, while ormosilane was added as a binder for the WO_3 in the photoelectrochromic device. After sintering of the dip-coated layer, only 2 % of Si is left from the ormosilane. IR spectral analysis confirmed that the addition of binder leads to the partial amorphisation of the monoclinic WO_3 grains [13]. The WO_3 layer for the photoelectrochromic device was dip-coated with a TiO_2 sol after sintering the WO_3 layer. The structural analysis confirmed that TiO_2 and SiO_2 are present in the amorphous WO_3 phase surrounding the WO_3 crystalline core [10]. Therefore the two WO_3 layers are similar concerning the crystalline part, but in the WO_3 layer used in the photoelectrochromic device, also an electrochemically active amorphous WO_3 phase is present. We performed the electrochemical potential measurements and ex-situ IR spectroscopy of the photoelectrochromic WO_3 layer in the same way as reported in [12].

We studied phase transitions of the WO_3 layer applied in the photoelectrochromic device using ex-situ IR spectro-electrochemical measurements and by analysing the XRD spectra of the layers charged to different extents. Characterisation of the photoelectrochromic devices confirmed that the voltage curves of the devices during the colouring or self-bleaching processes also resemble phase transitions that take place in electrochromic WO_3 layers.

2. EXPERIMENTAL

2.1 Sample Preparation

Transparent nano-porous TiO_2 and WO_3 layers were prepared using the following sol-gel techniques.

Peroxopolytungstic (P-PTA) sols were made by dissolving tungsten powder in hydrogen peroxide followed by thermal condensation in ethanol. For detailed information, see [14]. Ormosil precursors were made by an acylation reaction between isocianatopropyltriethoxy silane and diaminopolypropylene glycol 4000 in tetrahydrofurane as previously reported [15]. One mol % of ormosil precursor diluted in ethanol was added to the P-PTA sol. During stirring for 30 minutes, an ormosil network was formed by the hydrolysation-condensation reactions. To make TiO_2 layers, Ti (IV) isopropoxide was added to 10 ml of ethanol solution containing 2.6 g of ethyl acetoacetate. Separately, 1 g of ormosil (see above) was dissolved in 10 ml of ethanol and hydrolysation-condensation reactions were catalysed with 0.1 ml 0.1M HCl. After 30 minutes of stirring, the Ti solution was added and the solution was further stirred for 30 minutes.

A TCO (F:SnO_2) coated glass plate from Pilkington was covered by dip-coating first with WO_3, then with TiO_2 sol, and sintered in between and afterwards at 450°C for 30 min. The thickness of the TiO_2 layer was about 150 nm, and of the WO_3 layer about 500 nm. The Pt layer was sputtered with a mean thickness of about 2 nm. The dye (Ru 535 bis-TBA from Solaronix) was deposited by soaking the TCO/WO_3/TiO_2 layers in a solution of the dye in ethanol. The area of the samples was 5*5 cm^2. If not stated otherwise, the electrolyte was 0.5 M LiI and 0.005 M I_2 in propylene carbonate. Silicone film of 0.5 or 1 mm thickness was used as a spacer between the electrodes. The samples were sealed with acrylic adhesive.

To estimate the density and the porosity of the WO_3 layer, a thick WO_3 layer was prepared on aluminium foil as described in [16]. The volume and weight of the layer gave a density of 3.7g/cm^3. Non porous WO_3 has a density of 7.16 g/cm^3 [1]. Thus we concluded that the porosity is about 50%.

2.2 Characterisation of the Photoelectrochromic Devices

For characterising the kinetics of colouring during illumination and bleaching in the dark, we needed to have an experimental set-up, which measures the transmittance in the same way in

both cases. For this, we developed the set-up illustrated in fig. 4. A halogen lamp illuminates the photoelectrochromic sample, and the intensity of the transmitted light is detected by a silicon photodiode. The light intensity of the halogen lamp on the surface of the photoelectrochromic cell corresponds to 1 sun (1000W/m^2), taking into account the mismatch factor of dye solar cells. The two electrodes of the photoelectrochromic device are connected via a variable shunt resistance and a switch. For all configurations, the TiO_2 layer is always directed towards the lamp, so that the colouring of the WO_3 does not alter the light intensity on the TiO_2.

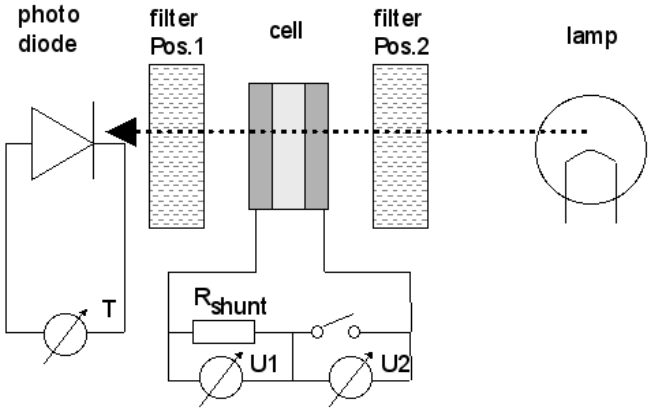

Figure 4: Experimental set-up for the characterisation of the kinetics of the colouring and bleaching process. T: transmittance, U1: corresponds to the current with switch closed, U2 corresponds to voltage with switch open. The TiO_2 layer faces toward the lamp. The filter is either in position 1 (cell illuminated) or in position 2 (cell in the dark).

The shunt resistance was chosen to be 10 Ω, which is similar to the resistance of the TCO layer. With this configuration, the voltage in the open circuit state and the current in the short circuit state were measured. For the dark state, an optical filter was placed between the lamp and the sample. This filter is transparent only in the range of the spectrum (above 715 nm) where the dye is not sensitive and no electrons are excited, as we demonstrated by spectral response measurements. (The portion of the spectral response of a dye solar cell transmitted through the filter is below 1%.) It was necessary to install several collimators in order to suppress scattered light from the environment. For the illuminated state, the filter was removed and placed between the sample and the photodiode detector. In this way, the optical signal is the same for both filter positions, and the transmittance signals for the dark and illuminated states are equivalent.

The measured value of the transmittance is a convolution of the spectra of the halogen lamp, the filter and the photodiode. In order to calculate the visible (or solar) transmittance from the measured value of the transmittance, the set-up was calibrated in the following way: A photoelectrochromic device was coloured to different extents by applying different voltages (0V, 0.3V, 0.4V, 0.5V, 0.6V, 0.7V) for 30 min, so that an equilibrium state was achieved. While holding this voltage with the potentiostat, the transmittance was measured with our set-up and immediately afterwards with a Perkin-Elmer 330 spectrometer which took the spectrum between 320 and 2000 nm. The visible (and solar) transmittance and optical density were calculated from these spectra. The visible (solar) optical density plotted versus the optical density as measured with our set-up shows a linear dependence to a good approximation. A linear fit gave a simple equation to calculate the visible (solar) optical density from the values determined with our set-up.

These calibration measurements were made with a special photoelectrochromic cell which was made without the dye. Coloured by an external voltage, this special cell has the same transmittance spectrum as the normal photoelectrochromic cell coloured by illumination, because the amount of dye in the normal cell is very low. Using this special cell for the calibration had the advantage that the measured transmittance is not influenced by the different light conditions inside the spectrometer and in our set-up.

The condition for this calibration is that the shape of the transmittance spectrum is independent of the degree of coloration. This condition is fulfilled because the dependence of the optical density on the charge is linear: The coloration efficiency C_E, defined as the change in optical density (OD) with the amount of charge inserted (Q), is independent of the intercalation degree x [8]. On the other hand, the optical density represents the intercalation degree x (x = number of intercalated Li^+ ions or injected electrons per W atom in the WO_3):

$$x = \frac{M_{WO_3}}{e_o N_A \rho L C_E}\, OD \approx 0.13\, OD \qquad (1)$$

M_{WO_3}: molar mass of WO_3, e_0: elementary charge, N_A: Avogadro's number, ρ: density of our nano-porous WO_3 (ρ=3.7g/cm^3), L: thickness of WO_3 layer (L=500nm), C_E=100cm^2/C.

Long-duration transmittance measurements of self-bleaching in the dark under open circuit conditions were made with a light-emitting diode with an intensity maximum at a wavelength of 655 nm without any filters. This light-emitting diode was switched on once every minute for a short measurement so that it did not influence the coloration of the photoelectrochromic device.

2.3 Characterisation of the Layers

The electrochemical potential of WO_3 layers during galvanostatic intercalation was measured using an EG&G PAR 273 computer-controlled potentiostat-galvanostat. A three-electrode sys-

tem was employed using a Pt rod as a counter electrode and a modified Ag/AgCl electrode [17] as a reference electrode for aprotic electrolytes (1 M $LiClO_4$ in propylene carbonate).

IR spectra of films were obtained using a FT-IR Perkin-Elmer 2000 spectrometer (spectral range 8000 – 400 cm^{-1}). The films were deposited onto 0.5 mm thick silicon wafers (p type, <1-0-0>), which were polished on both sides and had an electrical resistivity of 10-20 Ωcm. We used silicon wafers for the background correction. Prior to the electrochemical measurements, the uncoated surface of the Si wafer was cleaned with HF and an In-Ga alloy was applied to achieve better electrical contact. For ex-situ spectro-electrochemical measurements, films were galvanostatically charged and discharged in the range 0<x<0.5 with a current density of ±50 $\mu A/cm^2$. Different potential barriers were used when charging the WO_3 films to stop the measurements when a desired x was reached. After charging and discharging, the films were transferred from the electrochemical cell to the sample compartment of the IR spectrometer, which was purged with dry nitrogen gas.

3. RESULTS AND DISCUSSION

3.1 Phase Transitions in the Separate Layers

We measured the electrochemical potential of the WO_3 layers on the TCO substrate during galvanostatic Li^+ intercalation (fig.5). In the electrochemical potential, the typical steps for phase transitions are observed, as described above.

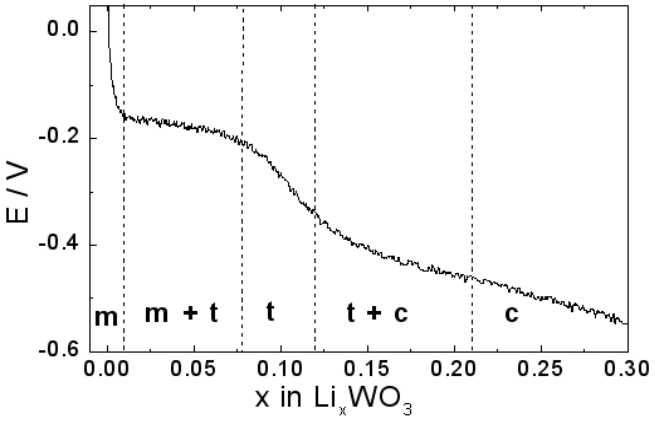

Figure 5: Electrochemical potential E of the WO_3 layer versus Ag/AgCl depending on the intercalation degree x, measured during galvanostatically charging of the WO_3. Electrolyte: 1 M $LiClO_4$ in propylene carbonate, m: monoclinic, t: tetragonal, c: cubic

The WO_3 layers were deposited onto silicon wafers polished on both sides using the same procedure as described in the "Experimental" section. The layers were galvanostatically charged in 1 M $LiClO_4$/ propylene carbonate electrolyte up to an intercalation degree of x = 0.3 (x = number of injected electrons per W atom). IR spectra were taken before and after intercalation and are shown in fig. 6. The IR spectrum of the as-deposited layer exhibits two main bands at 740 and 805 cm^{-1}. They are typical for monoclinic WO_3. Additionally some shoulder bands can be seen. Deconvolution analysis performed on the IR spectrum showed the presence of the bands that correspond to W-O-W vibrational modes characteristic for the amorphous hydrated WO_3 phase [13]. The IR spectrum of the electrochemically coloured WO_3 layer (x around 0.3) revealed the transformation of both main bands to a single band peaking at 780 cm^{-1}, the appearance of an additional band at 939 cm^{-1}, and a strong quasi-free electron absorption over the whole IR range. This transformation of the two main bands to one is characteristic for the transformation of the monoclinic to the cubic WO_3 phase [12]. The appearance of the band at 939 cm^{-1} is most probably due to the formation of terminal W=O bonds present in the outer part of the crystalline WO_3 core. Therefore we concluded that the presence of the amorphous shell does not influence the phase transitions characteristic for Li^+ insertion/extraction reactions of the monoclinic WO_3.

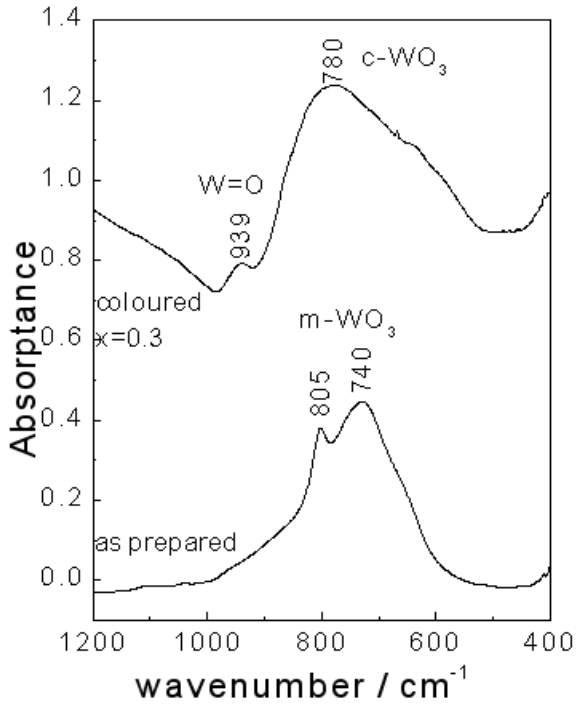

Figure 6: IR spectra of WO_3 on Si wafer in the bleached and the coloured states.

The IR spectra and the dependence of the electrochemical potential on the intercalation degree x are similar to that for the WO_3 layers prepared without ormosilane [12]. Both layers show the presence of the monoclinic WO_3phase [10] so they should

undergo the same phase transitions. We conclude that also the WO_3 crystals prepared with ormosilane transform from monoclinic through tetragonal to cubic structure during Li^+ intercalation. This is also in agreement with the results reported by Zhong et. al [11].

In fig. 5 the different phases in the different ranges of x are indicated. During the transformation of one phase to another, the electrochemical potential shows a plateau. In a pure phase, the potential decreases with increasing x.

3.2 The Voltage in the Photoelectrochromic Device

The density of photogenerated electrons in dye-sensitised TiO_2 in dye solar cells (in 1 sun in open circuit) is between $0.3*10^{17}/cm^3$ [18] and $2*10^{17}/cm^3$ [19]. In coloured WO_3 it is $8*10^{21}/cm^3$ (calculated from the density of WO_3 (7.2 g/cm^3) and the molar mass (232 g/mol) for 0.4 Li^+ ions per W atom). If we take into account the porosity of 50% of the WO_3, the electron density is halved. Because the electron density in WO_3 is 20000 times higher than in TiO_2, the electrochemical potential of both layers is dominated by the WO_3. This can be seen also in the time dependence of the open circuit voltage of the photoelectrochromic device. The electrons from TiO_2 are injected nearly completely into the WO_3. The loss reactions from the TiO_2 to the electrolyte can be neglected [9]. Under illumination the electrochemical potential in the TiO_2 is increasing very fast (equilibrium value of open circuit voltage is reached after approximately 0.5 s [20]). The electrons are injected into the WO_3 and the electrochemical potential in WO_3 is increasing according to equation (3). But in the WO_3 this takes much longer, U_{OC} reaches equilibrium after 20 min.

In the photoelectrochromic device, the Pt electrode in the presence of the redox couple I^-/I_3^- acts as a reference electrode under open circuit conditions. The changes in the potential during colouring due to the changes in the ion concentrations in the Nernst equation

$$\Delta V = \frac{[I_3^-]/[I_3^-]_{st}}{[I^-]/[I^-]_{st}} \qquad (2)$$

$[I_3^-]_{st}$,$[I^-]_{st}$: concentrations of I_3^- and I^- in the standard state, k_B: Boltzmann constant, T: temperature)

are only about 3 mV and can be neglected.

So if the measurement is made under equilibrium conditions (e.g. self-bleaching measurements), the open circuit voltage of the photoelectrochromic cell represents the electrochemical potential of the WO_3 layer. It is described by equation (3) and contains the influence of Li^+ and electrons.

3.3 Phase Transitions in the Photoelectrchromic Device

In fig. 7, a typical measurement of optical density and open circuit voltage of a photoelectrochromic cell during coloration under 1 sun illumination is shown. The optical density increases continuously, while the voltage increases rapidly during the first minute, reaches a maximum and then decreases slightly. On first inspection, this appear to be a contradiction. The increasing optical density shows that the intercalation degree x, defined as the number of injected electrons per W atom in the WO_3 layer, is increasing. On the other hand,

$$E(x) = a + bx - \frac{k_B T}{e_o} \ln\left(\frac{x}{1-x}\right) \qquad (3)$$

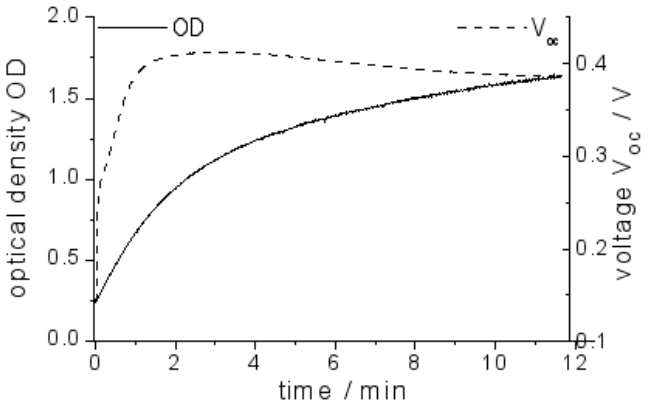

Figure 7: Coloration of the photoelectrochromic device in open circuit with 1000 W/m^2 (1 sun) illumination.

(a,b: constants) postulates that the electrochemical potential E and the voltage are also increasing continuously.

The constant a in equation (3) contains the energies for the reduction of W^{6+}, the interactions between W atoms of different oxidation levels, and of bonding between O and cations. The linear part is determined by the interaction between W atoms and intercalated cations, and the logarithmic part by the entropy. The equation is also supported by [19, 20, 2].

In the following we will explain this behaviour on the basis of the phase transition in the WO_3 layer:

In fig. 8, a measurement of self-bleaching is shown. The photoelectrochromic cell was first coloured under open circuit conditions under 1 sun illumination (as shown in fig. 7**)** and afterwards the open circuit voltage and the transmittance were measured in the dark. The bleaching of the WO_3 layer is possible then only via loss reactions (mainly the recombination of elec-

trons from the WO_3 layer with the I_3^- in the electrolyte [9]) and is therefore very slow.

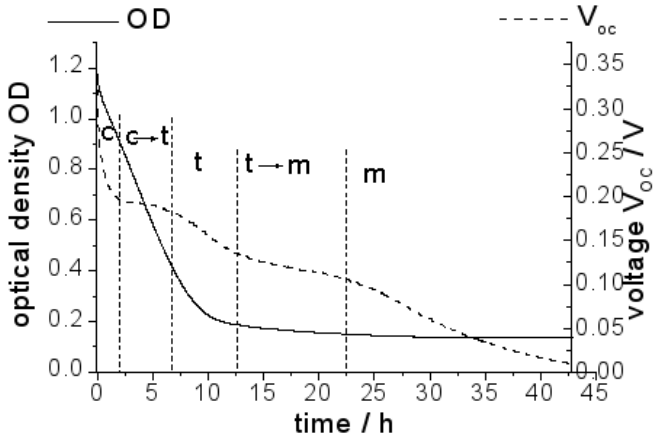

Figure 8: Self-bleaching in the dark in open circuit (optical density for 655 nm). c: cubic, t: tetragonal, m: monoclinic.

The steps in the open circuit voltage are of great interest. Qualitatively, they look similar to the steps in the electrochemical potential of the WO_3 layer as shown in fig. 5. The open circuit voltage of the photoelectrochromic cell is corresponding here to the equilibrium potential of the WO_3 versus the Pt electrode. The plateau in the voltage curve occur during phase transition, while the voltage decreases if a single phase is present. The optical density decreases continuously.

In contrast to the coloration under illumination, the self-bleaching is so slow that it can be considered as measurement under equilibrium conditions. The loss current which lead to the self-bleaching are close to zero (between 500 and 10 nA/cm^2).

In fig. 9, the voltage is plotted versus the intercalation degree x. The intercalation degree x is calculated from the optical density OD according to equation (1).

Two measurements are shown in this figure: The coloration of fig. 7 and the self-bleaching of fig. 8.

For lower values of x, the dependence of the voltage on x resembles the dependence of equation (3). For the self-bleaching, a broad plateau is observed; during the phase transition the voltage stays nearly constant over a broad range of x. The second plateau, which is clearly formed in fig. 8, is not visible in fig. 9 because the range of x for the second phase transition is very narrow (approximately between x=0.004 and 0.006), although it takes some hours in fig. 8. Only the different nearly linear ranges of the pure tetragonal and monoclinic phases give information about this phase transition.

A very interesting result of fig. 9 is the hysteresis between

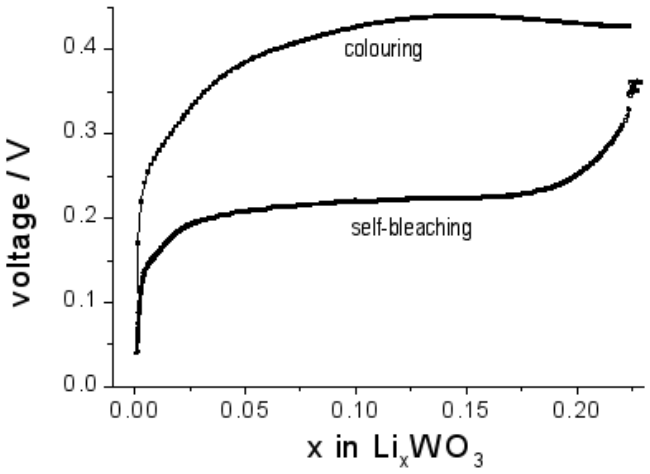

Figure 9: Open circuit voltage of the photoelectrochromic device depending on x for colouring with 1 sun illumination (no equilibrium conditions) and for self-bleaching in the dark (equilibrium conditions). The self-bleaching is just a different plot from the measurement shown in fig. 8. The broad plateau (0.05<x<0.17) corresponds to the transition between the cubic and the tetragonal phase. The transition between tetragonal and monoclinic phase takes place in such a narrow range that no plateau is formed.

colouring and self-bleaching. The voltage at one value of x is much higher for colouring than for bleaching. This observation is consistent with the experiments of [11] mentioned earlier.

We suggest the following interpretation for the unusual shape of the voltage profile during colouring. In this interpretation we use expressions about how fast the phase transition is compared to other processes. The speed of the phase transition we define as the number of W atoms changing from phase i to phase i+1 per second.

We assume a voltage curve corresponding to equation (3) for each phase: $U_i = a_i + b_i x_i - \frac{k_B T}{e_o} \ln\left(\frac{x_i}{1-x_i}\right)$, i=1, 2, 3 as indices of the three phases

The intercalation degree x_i of phase i is $x_i = \frac{N_{Li,i}}{N_{W,i}}$,

$N_{Li,i}$: number of intercalated Li^+ cations in phase i

$N_{W,i}$: number W atoms in phase i

$N_{W,tot}$: total number of W atoms

The optical density is proportional to the total intercalation degree

$$x = x_1 \frac{N_{W,1}}{N_{W,total}} + x_2 \frac{N_{W,2}}{N_{W,total}} + x_3 \frac{N_{W,3}}{N_{W,total}}$$

In fig. 10, a schematic illustration of the phase transition during colouring is made.

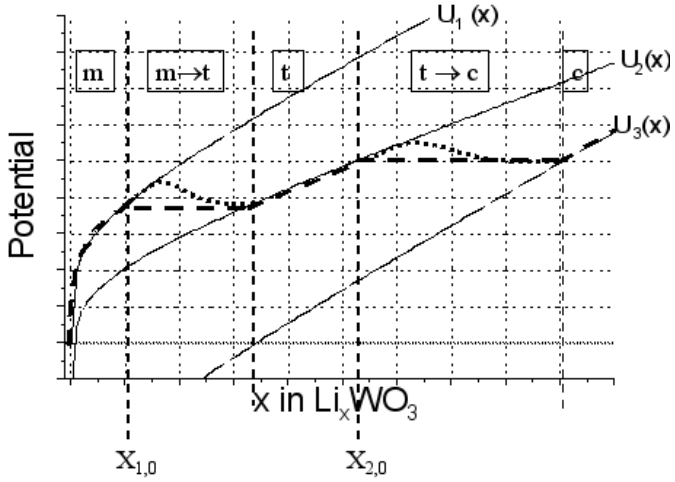

Figure 10: Schematic illustration of the effects of the phase transition on the voltage.

For small x, as long as the crystal structure is pure monoclinic, the potential follows the curve U_1. When a critical value $x_{1,0}$ is reached, the phase transition to the tetragonal phase starts [11]. The diffusion of the Li^+ ions (and of the electrons even more) in the WO_3 and in the electrolyte in the pores is fast compared to the phase transition. This means that voltage differences between the phases can be balanced immediately by electron and Li^+ exchange. During the phase transition, the voltages in phase 1 and phase 2 are always equal.

If x is increased very slowly, so that the intercalation of charges is slow compared to the phase transition, the potential is constant until all crystals have changed their structure. Then the potential follows the curve of the tetragonal phase U_2, which is linear in this range of x. During the phase transition, the intercalation degree in the monoclinic phase x_1 is always smaller than $x_{1,0}$ and the intercalation degree x_2 of the tetragonal phase is higher than $x_{1,0}$. While x_1 and x_2 stay constant, the total intercalation degree x and therefore also the optical density increase, because more and more WO_3 crystals change to the tetragonal phase.

If the intercalation is fast compared to the phase transition, x_1 becomes higher than $x_{1,0}$, because not all of the injected charges per time unit can be intercalated in the second phase. x_1 and x_2 increase. The potential continues to follow the monoclinic curve, until the increasing amount of WO_3 in the second phase leads to more intercalation of Li^+ in the second phase. x_1 and x_2 decline and the voltage decreases. This is an explanation for the decrease of the voltage after reaching a maximum. Another possible explanation is that the exchange current density of the loss reaction is increasing with x or with the second phase, so that the loss reactions are becoming so fast for high x that the number of intercalated charge carriers per time unit is decreasing and x_1 and x_2 are decreasing. Then also the voltage drops. However, x continues to grow, as we can see in the optical density.

Analogous considerations can be made for the second and third phases.

If the phase transitions between the first and second phases ($x_{1,0}$), and between the second and third phases ($x_{2,0}$), are close together (that means that $x_{2,0}$ is approximately the value of x where the maximum would be formed), the first maximum in fig. 10 is not formed, but is transformed to an inflection point.

For self-bleaching, analogous considerations can be made for decreasing x. The parameters a_i and b_i, which determine the gradient of the voltage in the pure phase, and $x_{i,0}$, which determines the start of phase transition, are different. This is in accordance with [11]. (A detailed discussion of this interpretation with the help of a mathematical model of the coloration and self-bleaching processes will be published soon.)

This interpretation is confirmed by variation of the light intensity: The dependence on x of the open circuit voltage of the photoelectrochromic device under illumination with different intensities is shown in Fig. 11. For low light intensity, the electron injection is slow enough for the phase transition to keep pace. The voltage increases continuously with increasing x. The transitions between the monoclinic and the tetragonal phases and between the tetragonal and the cubic phases cause inflection points.

For high light intensity, the electron injection is so fast that the phase transition cannot keep pace. The voltage increases until a maximum and then decreases again. This maximum is a result of the transitions between the tetragonal and the cubic phase. The transitions between the monoclinic and the tetragonal phase cause an inflection point.

4. CONCLUSION

The phase transitions in the crystalline core of the WO_3 particles were investigated for the separate WO_3 layers by measurement of the electrochemical potential, IR spectra and X-ray diffraction. It was shown that the initially monoclinic core of the WO_3 particles is transformed through tetragonal to cubic structure when electrons and Li^+ cations are intercalated. It was demonstrated that the same phase transitions take place in the complete photoelectrochromic device when the intercala-

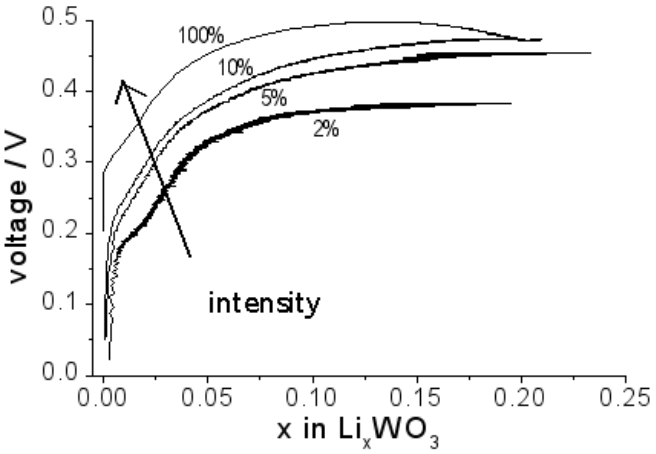

Figure 11: Coloration of the photoelectrochromic device in open circuit under illumination with different light intensities. 100% corresponds to an intensity of 1000 W/m^2 (1sun).

tion is powered by illumination. The unusual time dependence of the open circuit voltage, which shows inflection points and maxima during switching of the photoelectrochromic device, while the optical density is increasing (respectively decreasing) monotonously, was explained by the observed phase transitions.

5. ACKNOWLEDGMENTS

This work was supported financially by the University of Freiburg, and the German Ministry of Education and Research BMBF. The Ministry of Education, Science and Sport of the Republic of Slovenia is also acknowledged for financial support (Z2-3524).

REFERENCES

[1] C.G. Granqvist, “Handbook on Inorganic Electrochromic Materials”, ELSEVIER SCIENCE B.V., Amsterdam, Netherlands, 1995.

[2] C.G. Granqvist, Solar Energy Materials and Solar Cells 60, 201 (2000).

[3] B. O’Regan, M. Grätzel, Nature 353, 737 (1991).

[4] K. Kalyanasundaram, M. Grätzel, Coordination Chemistry Reviews 77, 347 (1998).

[5] C. Bechinger, S. Ferrere, A. Zaban, J. Sprague, B. A. Gregg, Nature 383, 608 (1996).

[6] G. Teowee, T. Gudgel, K. McCarthy, A. Agrawal, P. Allemand, J. Cronin, Electrochim. Acta 44, 3017 (1999).

[7] F. Pichot, S. Ferrere, R. J. Pitts, B. A. Gregg, J. Electrochem. Soc. 146 (11), 4324 (1999).

[8] A. Hauch A. Georg, S. Baumgärtner, U. Opara Krašovec, B. Orel, Electrochim. Acta 46, 2131 (2001).

[9] A. Hauch, A. Georg, U. Opara Krašovec, B. Orel, J. Electrochem. Soc. 149 (9), H159 (2002).

[10] U. Opara Krašovec, Anneke Georg, Andreas Georg, G. Dražič, submitted to the Journal of Sol-Gel Science and Technology.

[11] Q. Zhong, J.R. Dahn, K. Colbow, Physical Review B 46, N° 4, 2554 (1992).

[12] U. Opara Krašovec, A. Šurca Vuk, B. Orel, Electrochim. Acta 46, 1921 (2001).

[13] U. Opara Krašovec, R. Ješe, B. Orel, J. Grdadolnik, G. Dražič, Monatshefte für Chemie (Chemical Monthly) 133, 1115 (2002).

[14] B. Orel, U. Opara Krašovec, U. Lavrenčič Štangar, P. Judeinstein, Journal of Sol-Gel Science and Tecnology 11, 87 (1998).

[15] N. Grošelj, M. Gaberšček, U. Opara Krašovec, B. Orel, G. Dražič, P. Judeinstein, Solid State Ionics 125, 125 (1999).

[16] A. Hauch, A. Georg, U. Opara Krašovec, B. Orel, J. Electrochem. Soc. 149 (9), A1208 (2002).

[17] A. Šurca, B. Orel, G. Dražič, B. Pihlar, J. Electrochem. Soc. 146, 232 (1999).

[18] J. Ferber, R. Stangl, J. Luther, Solar Energy Materials and Solar Cells 53, 29 (1998).

[19] S. Kambe, S. Nakade, T. Kitamura, Y. Wada, S. Yanagida, J. Phys. Chem. B 106, 2967 (2002)

[20] N.W. Duffy, L.M. Peter, R.M.G. Rajapakse, K.G.U. Wijayantha, Electrochemistry Communications 2, 658 (2000)

[21] R.S. Crandall, P.J. Wojtowicz and B.W. Faughnan, Solid State Communications 18, 1409 (1976).

[22] M.L. Hitchman, J. Electroanal. Chem. 85, 135 (1977)

[23] B. Reichman, A.J. Bard, J. Electrochem. Soc. 127, 241 (1980)